

ICFDP9-EG-263

CHARACTERISTICS OF JET ISSUING FROM CIRCULAR CYLINDER IN CROSS-AIR STREAM

A.M.R. ELBAZ
Assistant Professor,
Department of Mechanical
Engineering, Faculty of
Engineering, Ain Shams
University

M. A.NOSIER,
Professor, Department of
Mechanical Engineering, Faculty
of Engineering, Ain Shams
University

H.A. ABOTALEB
Assistant Lecturer, Department
of Mechanical Engineering,
Faculty of Engineering, Ain
Shams University

ABSTRACT

This research aims to study the characteristics of two dimensional jet issuing from circular cylinder in cross air stream at different velocity ratios and injection angles relative to the direction of main stream. The results show important effect of velocity ratio on flow development. The jet penetration is stronger for higher velocity ratio. Jets issuing at right angle to the main flow direction also have stronger penetration compared with jets issued at a smaller angle. Reducing the injection angle also increases turbulence downstream the cylinder. The correlation obtained for jet trajectory into the main stream for plane jet showed stronger penetration compared with published data for round jets. This behaviour is attributed to the fast decay of round jets compared with that of plane jets

KEYWORDS:

Turbulent Jets, Cross Flow, Cylinder Wake.

INTRODUCTION

The injection of fluid jet transversely into a moving stream is a basic configuration which finds application in many engineering fields. Examples include vertical takeoff and landing of air crafts, film cooling of gas turbine blades, environmental problems such as pollutant dispersion from chimneys or the discharge of effluents into the ocean as well as other applications. Enhancement of the mixing rate between jet and cross flow can lead to significant improvements of performance in most applications.

Because of its great practical significance, numerous previous experimental and theoretical studies have been carried out on the jet in cross flow problem, Haniu and Ramaprian (1983), Ramaprian and Haniu (1989), Vincenti et al (2002) and Kalita et.al. (2002). In all previously published literature the investigated flow involved either plane or round jets issuing from a plane surface which is parallel to the main stream. This configuration is applicable in some practical cases. However, in some other applications, e. g. steam humidifiers, the injected flow is issued from a circular surface (pipe) which is perpendicular to the main stream. In such configuration, the main stream interacts with the injected flow and the pipe wake. Despite its practical importance, no previous investigations are available in the published literature which documents flow behaviour in this configuration.

The injected jet behavior depends on the ratio between the jet velocity V_j and main stream velocity U_∞ ($R=V_j/ U_\infty$). The jet is deflected by the action of the main stream. The velocity ratio affects the resulting streamline curvature of the jet. The jet is classified as a strong jet if the velocity ratio is high. In this case the jet behaviour is similar to that injected into still ambient, Keffer and Baines (1963). For low velocity ratio, the jet is classified as weak jet and behaves like an asymptotic small defect wake.

The trajectory of the injected jet is defined by the location of the maximum velocity (Y_m) along jet path. The correlation between jet trajectory (for perpendicular injection) which includes the effects of jet diameter (d) and jet/cross-flow

velocity ratio (R) is proposed to take the following form for round jets (Kamotani and Greber (1974)):

$$(Ym/d) = 0.89 R^{0.94} (X/d)^{0.36} \quad (1)$$

where d is the jet orifice diameter.

The objective of the present work is to investigate the behaviour of two dimensional jets injected into a cross stream from a circular cylinder. The investigation includes jets of different velocity ratios ranging between 5 and 8. The measurements were performed for perpendicular injection as well as inclined injection.

2. EXPERIMENTAL SET-UP

The jet orifice used is two dimensional slot of 0.85 mm width and 60 mm long, created on hollow circular cylinder of 9.5 mm outer diameter, 7.5 mm inner diameter and 300 mm long. The cylinder was mounted across a wind tunnel test section of 300 mm width, 300 mm height and 600 mm length. The wind tunnel components are shown in figure 1 while the injected jet configuration is shown in figure 2.

The main stream velocity was varied between 8 m/s and 13.3 m/s, which are equivalent to cylinder Reynolds numbers between 4800 and 8000. The jet velocity was fixed at 69.7 m/s corresponding to jet Reynolds number of 3830. The injection angles used were 0° , 30° , 60° and 90° relative to the main stream direction. The experiments were carried out at three velocity ratios R of 5.2, 7.0 and 8.7.

The measurements of the mean velocity component in the direction of the main stream and its turbulence intensity were carried out by means of DANTEC single hot wire anemometer. In order to avoid the cylinder wake circulation zone, measurements started at a distance of 3.6 times the cylinder diameter which is equivalent to 40 times the slot width. Three other measuring stations were examined at 60, 80 and 100 times the slot width.

3. RESULTS

3.1 Mean Velocity Measurements

The measured normalized mean streamwise velocity profiles at different locations downstream the cylinder for $R=5.2$ and $\alpha=90^\circ$ are shown in figures 3 and 4. The streamwise coordinate X, and cross stream coordinate Y are normalized using the jet slot width W. The local mean velocity is normalized by the free stream velocity. As can be seen in the figures, the flow structure can be split into two zones; the jet zone where the local velocity is higher than the free stream velocity ($U/U_\infty > 1$) and the wake zone in which the velocity is lower than the free stream velocity ($U/U_\infty < 1$). Note that the jet is injected in the positive Y direction and at right angle to the main stream flow direction. The origin of both X and Y coincides with the centre of the cylinder.

The wake zone is generated due to the cylinder and the deflected jet simultaneously. As can be seen, the wake is asymmetric with respect to cylinder symmetry plane ($Y/W=0$). This is due to the fact that the major wake is generated by the deflected jet rather than the circular cylinder. The maximum velocity is observed above the symmetry plane. The value of the maximum velocity diminishes as the flow develops. At $X/W=80$ the positive jet nearly disappears and the flow is dominated by the wake structure.

Figures 5 and 6 show the measured normalized mean streamwise velocity profiles at different locations downstream the cylinder for $R=7$ and $\alpha=90^\circ$. In this case, stronger jet penetration can be observed. The wake size is relatively larger than that observed for $R=5.2$. The excess velocity characterizing the jet zone is still distinct even at $X/W=100$. At this location the maximum velocity in the jet region is 20 % higher than the free stream velocity. The location of the maximum velocity occurs at $Y/W > 50$ for all measurement stations. Similar trend can be observed for $R=8.7$ as shown in figures 7 and 8.

Figures 9-12 show the comparison between the measured profiles for different velocity ratios of jets injected at right angle to the main stream direction at different locations. The figures also include the measured profile for the cylinder wake without jet injection for comparison. The cross stream coordinate is normalized by the cylinder diameter d. The figures show that the wake profile has a noticeably lower momentum defect compared with all other cases. This confirms the fact that the wake generated by the deflected jet is more important than the cylinder wake in forming the developing flow. The cylinder wake is symmetric while the deflected jet wake is asymmetric. The figures also manifest the effect of jet velocity ratio on jet penetration. The location of the maximum velocity at all stations is shifted further away from the cylinder centreline for higher jet velocity. The peak velocity of each case is quite distinct as can be seen in figures 9 to 12. The width of the jet wake also increases as the velocity ratio increases. This behaviour is similar to that of jets injected from a flat surface. Regarding the lower wake, it is interesting to note that the measured velocity profiles are close to measurements in the free wake of the cylinder alone. The jet wake merges with the cylinder wake as the flow develops after $X/d=5.3$.

Figure 13 shows a comparison between mean streamwise velocity profiles for different injection angles at $X/W=100$ and $R=8.7$. The measurements show that reducing the injection angle results in less jet penetration into the main stream. The location of maximum velocity for $\alpha = 60^\circ$ is approximately at $Y/D = 4.5$ while that for $\alpha = 90^\circ$ is at $Y/D \sim 7$. For $\alpha = 60^\circ$ this location is at $Y/D \sim 4$. The reduced jet penetration is also accompanied with weaker jet decay. The highest jet velocity at $X/W = 100$ is that for the lowest jet injection angle of 30° .

There is no trace of the wake at this location since positive streamwise velocity is observed across the whole flow field. In this case the jet momentum excess in the streamwise direction outweighs the wake momentum defect.

Figure 14 shows a similar comparison between mean streamwise velocity profiles for different injection angles at $X/W=100$ and $R=5.2$. As can be seen in the figure, no wake is observed for $\alpha=30^\circ$. However, the wake is clear for $\alpha=60^\circ$ and $\alpha=90^\circ$.

The jet trajectory can be defined by the locus of maximum velocity (Y_m) at different downstream distances from the injection point. The trajectory of the jet is examined by plotting the location of the maximum streamwise velocity versus streamwise coordinate, X/W , in figure 15. The symbols included in the figure indicate measured data while the continuous lines are obtained from the correlation:

$$(Y_m/W) = 0.89 R^{1.01} (X/W)^{0.5} \quad (2)$$

This correlation is similar to equation 1 which was derived from round jet results, with slightly different constants. Figure 15 shows that the proposed correlation provides good agreement with the measured values of Y_m/W for different velocity ratios.

Figure 16 shows a comparison between the reported correlation for $\alpha=90^\circ$ for round jet issuing from a flat surface (equation 1) and the present correlation for plane jets issuing from a circular cylinder (equation 2), for $R=5.2$. As can be seen in the figure, plane jets issuing from circular cylinder penetrate the main stream more than circular jets issuing from a flat surface. This behavior is mainly associated with the shape of orifice. Since round jets decay faster than plane jets, Rodi (1975), the former type is expected to have a weaker penetration into the main stream than the latter.

Figure 17 shows the variation of jet trajectories for three injection angles of 90, 60 and 30 degrees, measured from the flow direction. The measurements show that as the injection angle decreases the location of the maximum velocity is lowered towards the centerline of the cylinder. The effect of changing the injection angle from 90 to 60 degrees on the trajectory is strong. However, weaker effect can be observed when the angle is changed from 60° and 30°. Similar trends can be observed for other velocity ratios as shown in figures 18 and 19 for $R=7$ and 8.7 , respectively.

3.2 Turbulence Measurements

The turbulence measurements were made using a single hot wire anemometer. This technique allows the measurements of fluctuations in one direction. In the present work only streamwise fluctuations were measured across the flow at different measurement locations.

Figures 20 and 21 show the measured distribution of streamwise turbulence fluctuations (root mean square value) normalized by the free stream velocity. In both figures the turbulence profiles have two distinct peaks. The first peak corresponds to the cylinder wake part of the flow which extends above cylinder centerline ($Y/W < 0$). The other peak corresponds to jet region. The peak turbulence in the jet region is nearly twice that in the wake region. This trend is observed in the near field only. At $X/W=80$ and 100 , the two peaks become closer which indicates that both flows tend to merge into one common wake flow, as observed in the mean velocity profiles at the same locations, (see figure 4 above).

The turbulence measurements for $R=8.7$ are shown in figures 22 and 23. As can be seen, the peak turbulence in the jet region is much higher in this case than that in the wake region. The peak turbulence intensity is also higher than that observed for $R=5.2$. At $X/W=100$, the jet region still has a noticeable peak turbulence intensity.

Figures 24 and 25 show the measured turbulence profiles for $R=8.7$ and injection angle = 60° . As can be seen in both figures, the small injection angle results in a high turbulence level in the jet region, compared with the 90° case. This results from the stronger shear generation in this case since the jet flow does not penetrate as deep as that of the 90° case, and thus retains a high centerline velocity for longer distance downstream. Far downstream, at $X/W=80$ and 100 , the measured profiles show a single peak. The flow in this case is closer to jet flow due to the weaker penetration into the flow.

4 CONCLUSIONS

The present paper presented mean flow and turbulence measurements in the downstream region of two dimensional jet injected in a cross stream. The jet was issued from a circular cylinder placed across the flow. Three jet injection velocity ratios were investigated, namely 5.2, 7 and 8.7. Mean flow measurements showed that the velocity ratio has a significant effect on jet trajectory. The correlation between jet trajectory and streamwise distance matching the present results is slightly different from that of round jets issuing into a cross stream from flat surface. The jet wake interaction with the cylinder wake was also noticed along the flow. The resulting wake of the jet in cross flow is much wider than the cylinder wake. Reducing the injection angle of the jet relative to the free stream flow direction has a strong effect on jet trajectory and turbulence intensity downstream the injection point.

NOMENCLATURE

- D** Cylinder diameter
- L** Plane jet slot length
- R** Injection velocity ratio ($r=v_j/u_\infty$)

Re_j Reynolds number of jet based on plane jet width ($\rho V_j w / \mu$)
Re_m Reynolds number based on cylinder diameter ($\rho V_j d / \mu$)
U Local velocity component in x-direction (u-component).
u' Local turbulence intensity component in x-direction.
U_∞ Velocity of tunnel flow (main flow)
V_j Velocity at jet exit (secondary flow)
W Plane jet slot width
X Streamwise coordinate measured from cylinder centerline
Y Cross stream coordinate measured from wake centerline

α Angle of secondary flow injection relative to main stream.
μ Viscosity
ρ Density

REFERENCES

1. Evanov V.V., 1959, "The Strong Burning of Layer Gases in the Furnace", ASTONCK National Publisher, DALIN.
2. Fan J. and Hua Q., 1992, "Numerical Prediction of a Rectangular Turbulent Jet in a Cross Flow", Chem. Eng. Comm., Vol. 117, pp. 293-306.
3. Fearn R.L. and Weston R.P., 1979, "Velocity Field of a Round Jet in a Cross Flow for Various Jet Injection Angles and Velocity Ratios", National Aeronautics and Space Administration, NASA Technical Paper 1506.
4. Haniu H. and Ramaprian B.R., 1989, "Studies on Two-Dimensional Curved Non-buoyant Jets in Cross Flow", Journal of Fluids Engineering Trans., ASME, vol. 111, pp. 78-86.
5. Heskestad G., 1965, "Hot wire measurements in a plane turbulent jet", J. Appl. Mech., 32, 721-734.
6. Kalita K., Dewan A. and Dass A.K., 2002, "Prediction of Turbulent Plane Jet in Crossflow", Numerical Heat Transfer, Part A, 41, pp. 101-111.
7. Kamotani Y. and Greber I., 1972, "Experiments on a Turbulent Jet in a Cross Flow", AIAA Journal., Vol. 10, No.11, pp. 1425-1429.
8. Kamotani Y. and Greber I., 1974, "Experiments on Confined Turbulent Jets in Cross Flow", National Aeronautics and Space Administration, NASA CR-2392.
9. Keffer J.F. and Baines W.D., 1963, "The Round Jet in a cross-Wind", J. Fluid Mech., pp.481-496.
10. Ramaprian B.R. and Haniu H., 1983, "Turbulence Measurements in Plane Jets and Plumes in Cross Flow", Technical Report No. 266, IIHR.
11. Rodi, W. 1975, A Review of Experimental Data of Uniform Density Free Turbulent Boundary Layers. In Studies in Convection, vol. 1, B. E. Launder (ed.), Academic Press, London.
12. Vincenti I., Guj G., Camussi R. and Giulietti E., 2002, "PIV study for the analysis of planar jets in cross-flow at low Reynolds number", Vasca Navale 79, 00146, Rome (Italy).

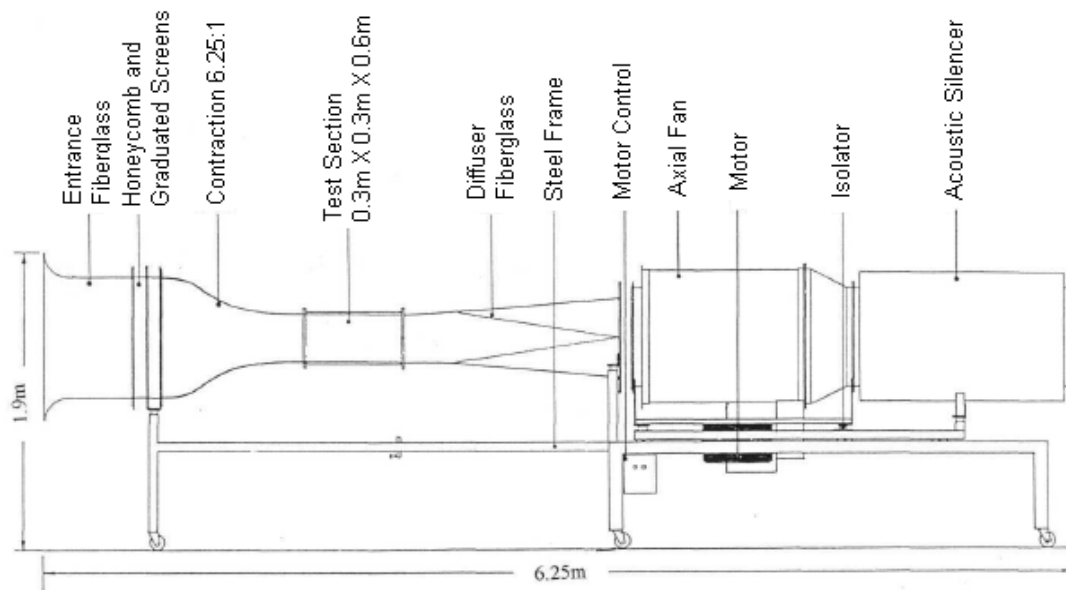


Figure 1: Open circuit wind tunnel.

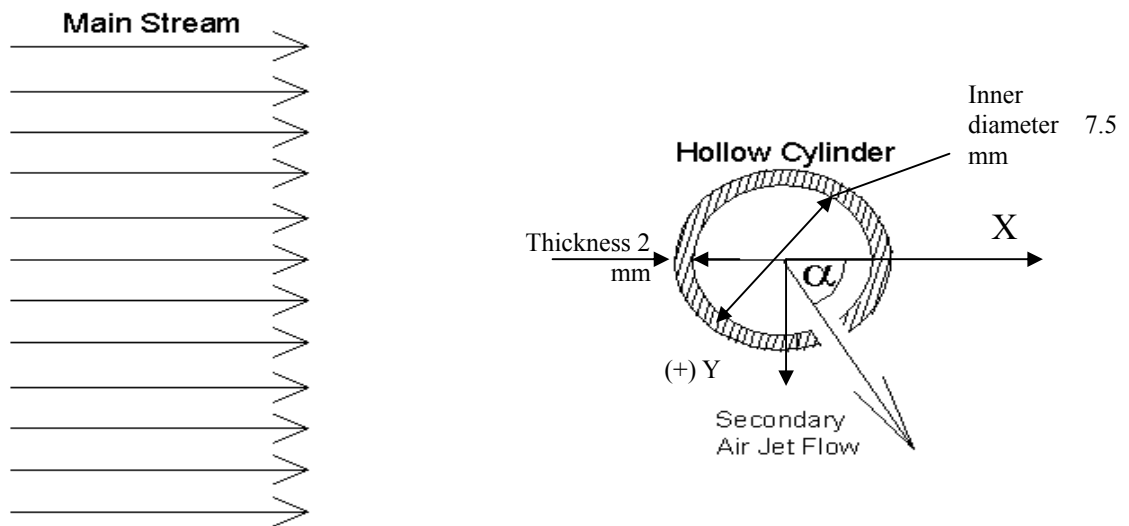


Figure 2: Jet issuing from circular cylinder in cross flow

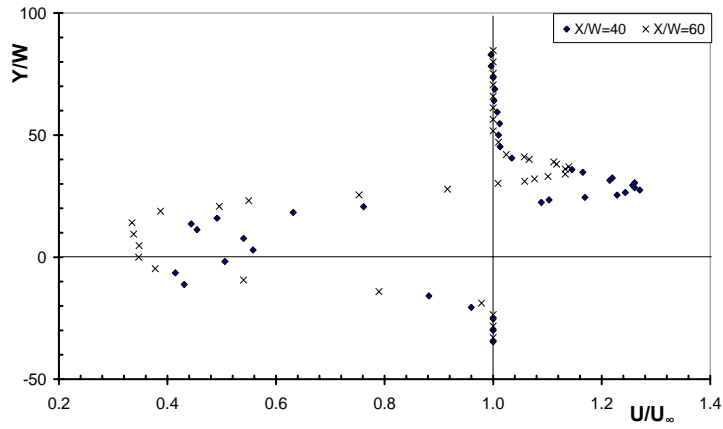


Figure 3: Mean streamwise velocity profiles downstream the cylinder, $R=5.2$ and $\alpha=90^\circ$. ($X/W=40, 60$)

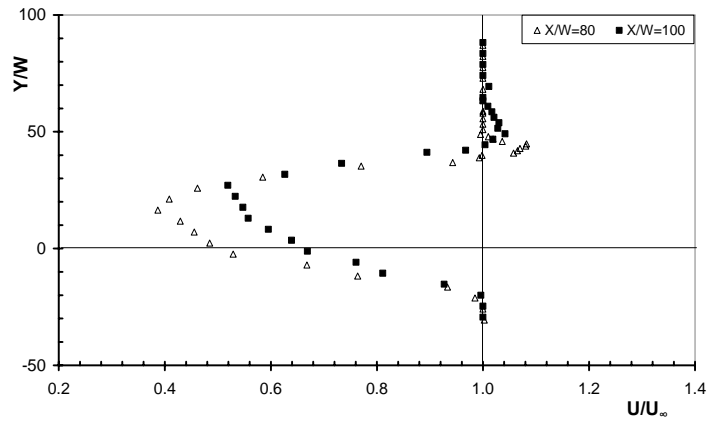


Figure 4: Mean streamwise velocity profiles downstream the cylinder, $R=5.2$ and $\alpha=90^\circ$. ($X/W=80, 100$)

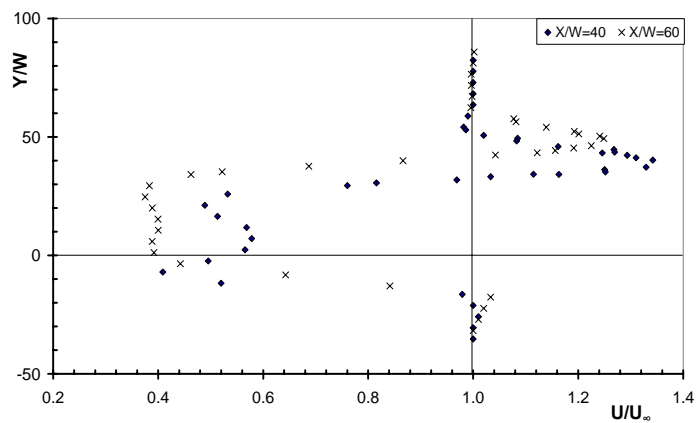


Figure 5: Mean streamwise velocity profiles downstream the cylinder, $R=7$ and $\alpha=90^\circ$. ($X/W=40, 60$)

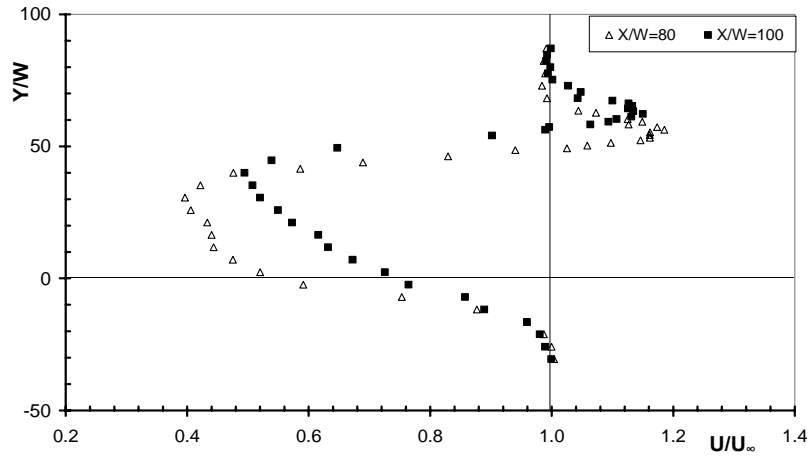


Figure 6: Mean streamwise velocity profiles downstream the cylinder, $R=7$ and $\alpha=90^\circ$. ($X/W=80, 100$)

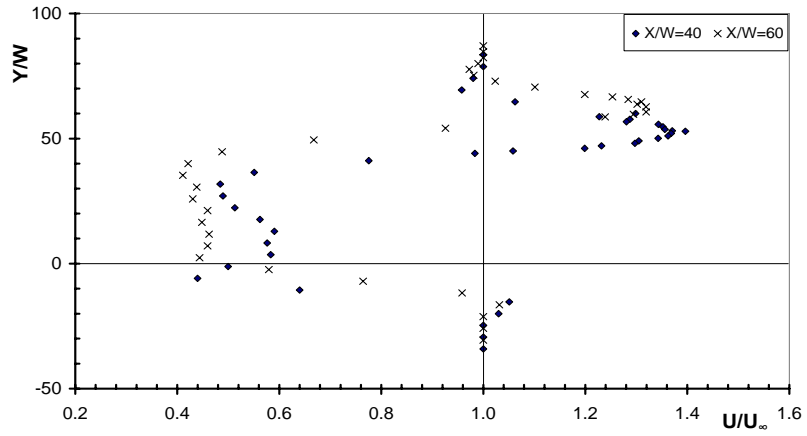


Figure 7: Mean streamwise velocity profiles downstream the cylinder, $R=8.7$ and $\alpha=90^\circ$. ($X/W=40, 60$)

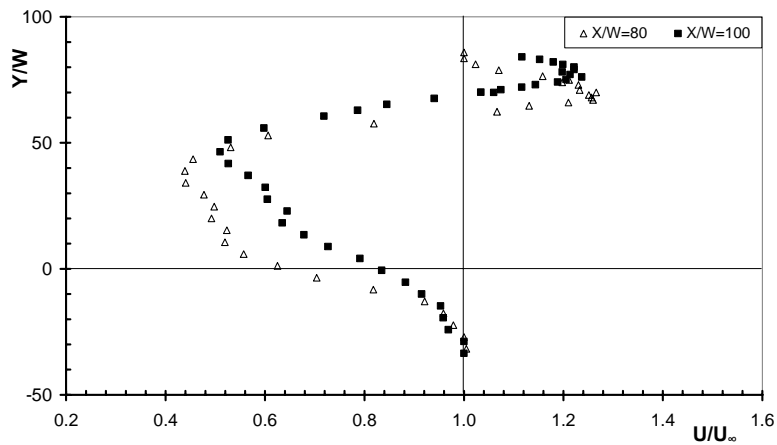


Figure 8: Mean streamwise velocity profiles downstream the cylinder, $R=8.7$ and $\alpha=90^\circ$. ($X/W=80, 100$)

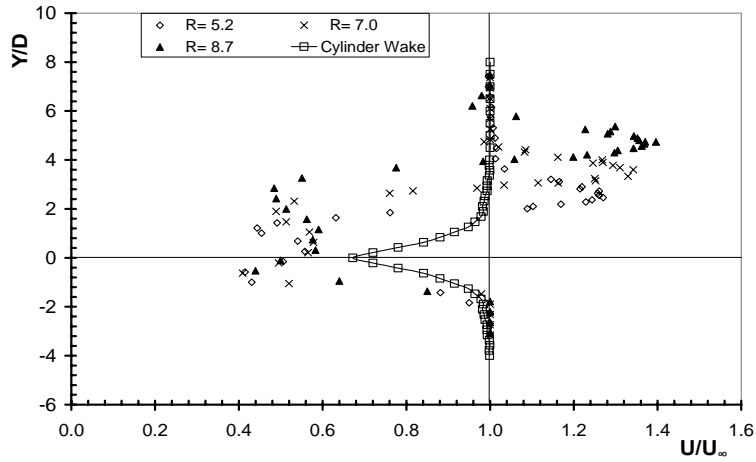


Figure 9: Comparison between mean streamwise velocity profiles for different velocity ratios at $X/W=40$ ($x/d=3.6$) and $\alpha=90^\circ$.

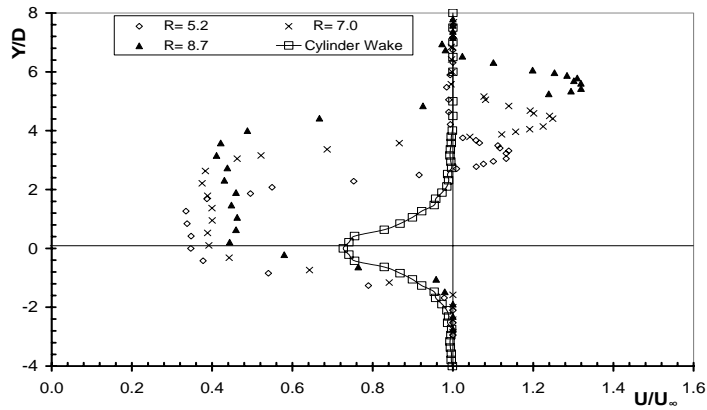


Figure 10: Comparison between mean streamwise velocity profiles for different velocity ratios at $X/W=60$ ($x/d=5.37$) and $\alpha=90^\circ$.

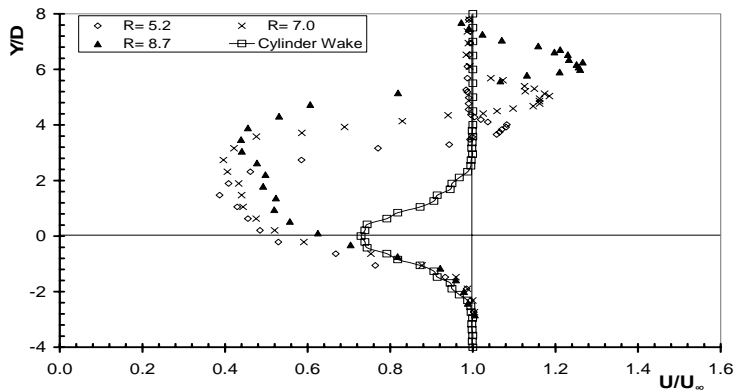


Figure 11: Comparison between mean streamwise velocity profiles for different velocity ratios at $X/W=80$ ($x/d=7.16$) and $\alpha=90^\circ$.

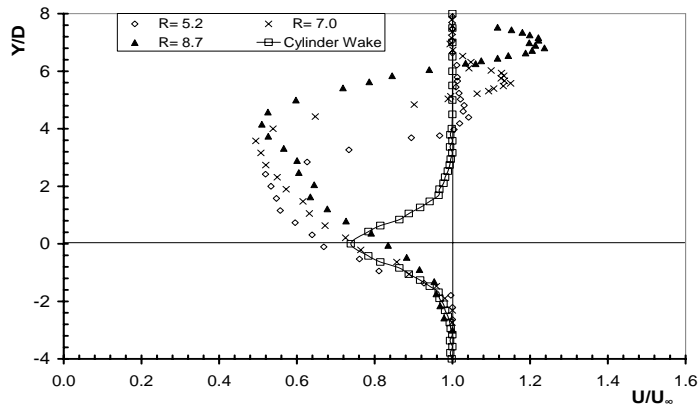


Figure 12: Comparison between mean streamwise velocity profiles for different velocity ratios at $X/W=100$ ($x/d=8.95$) and $\alpha=90^\circ$.

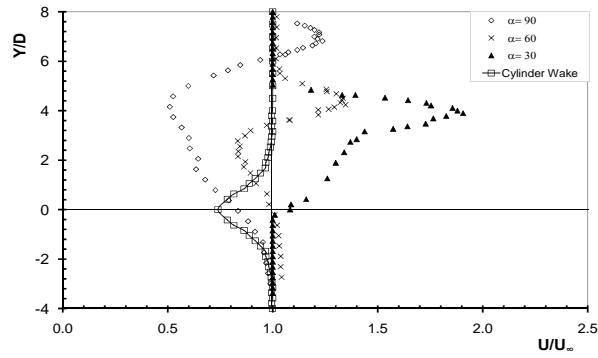


Figure 13: Comparison between mean streamwise velocity profiles for different injection angles at $X/W=100$ ($x/d=8.95$) and $R=8.7$.

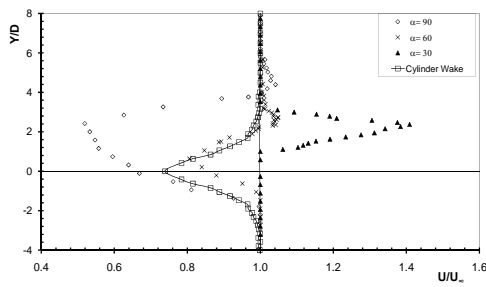


Figure 14: Comparison between mean streamwise velocity profiles for different injection angles at $X/W=100$ ($x/d=8.95$) and $R=5.2$.

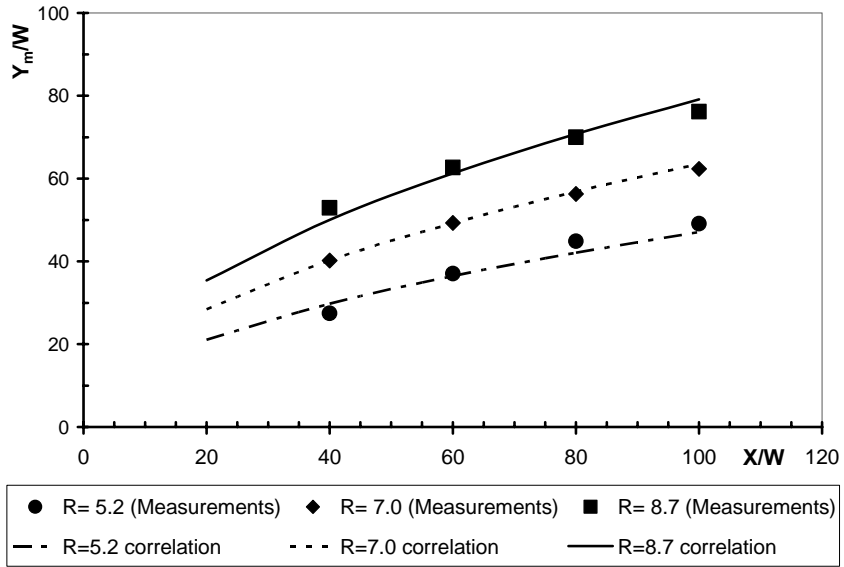


Figure 15: Trajectories of jet in cross flow at $\alpha=90^\circ$

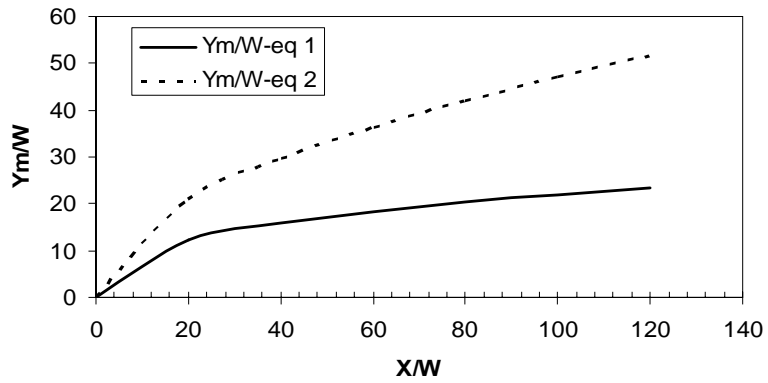


Figure 16: Comparison between jet trajectory correlations in equation 1 and equation 2

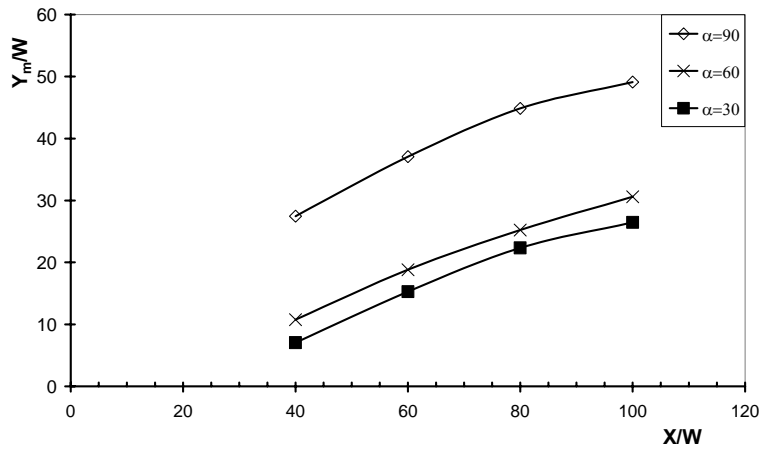


Figure 17: Effect of injection angle on jet trajectory (R=5.2).

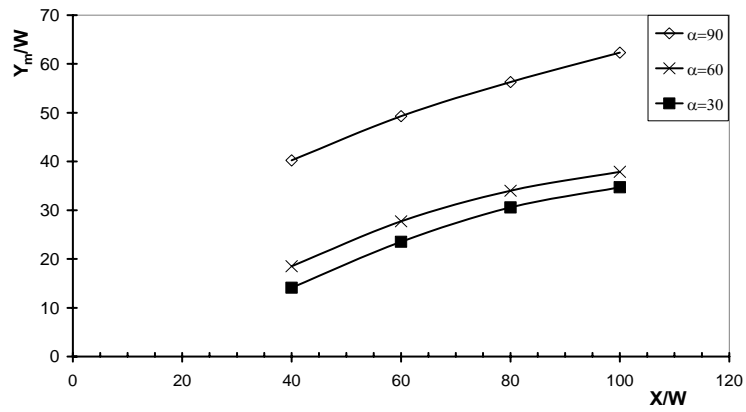


Figure 18: Effect of injection angle on jet trajectory (R=7).

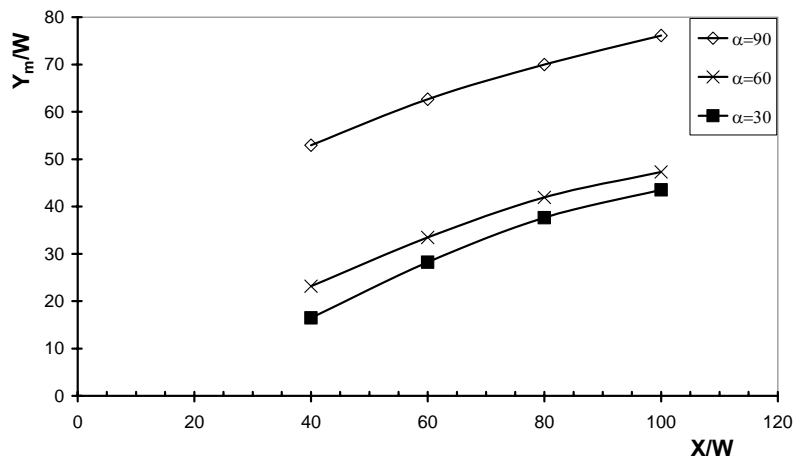


Figure 19: Effect of injection angle on jet trajectory (R=8.7).

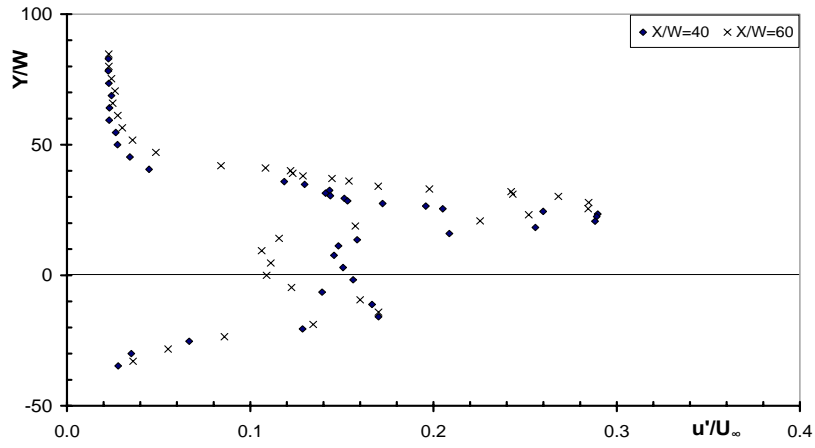


Figure 20 Turbulence streamwise fluctuations downstream the cylinder, $R=5.2$ and $\alpha=90^\circ$. ($X/W=40, 60$)

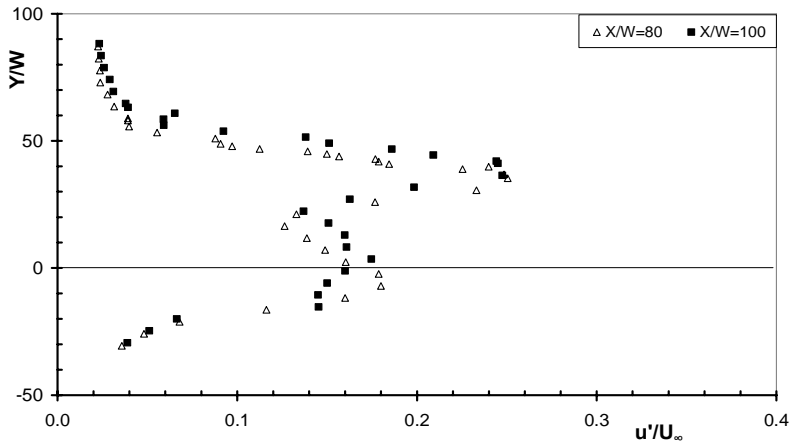


Figure 21 Turbulence streamwise fluctuations downstream the cylinder, $R=5.2$ and $\alpha=90^\circ$. ($X/W=80, 100$)

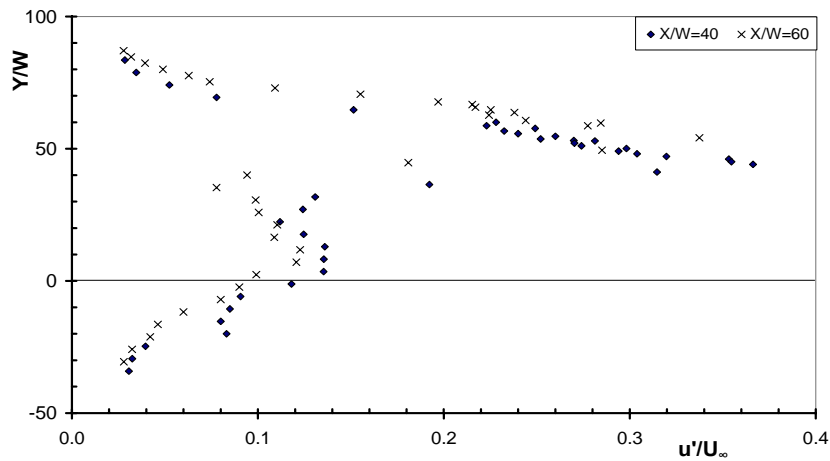


Figure 22 Turbulence streamwise fluctuations downstream the cylinder, $R=8.7$ and $\alpha=90^\circ$. ($X/W=40, 60$)

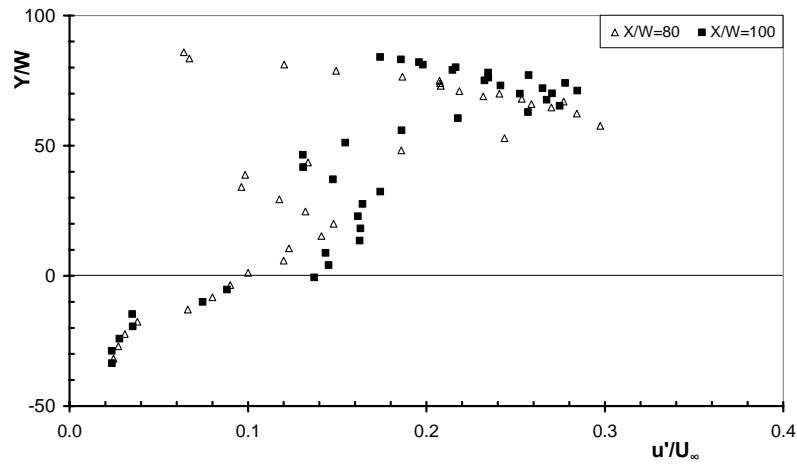


Figure 23 Turbulence streamwise fluctuations downstream the cylinder, $R=8.7$ and $\alpha=90^\circ$. ($X/W=80, 100$)

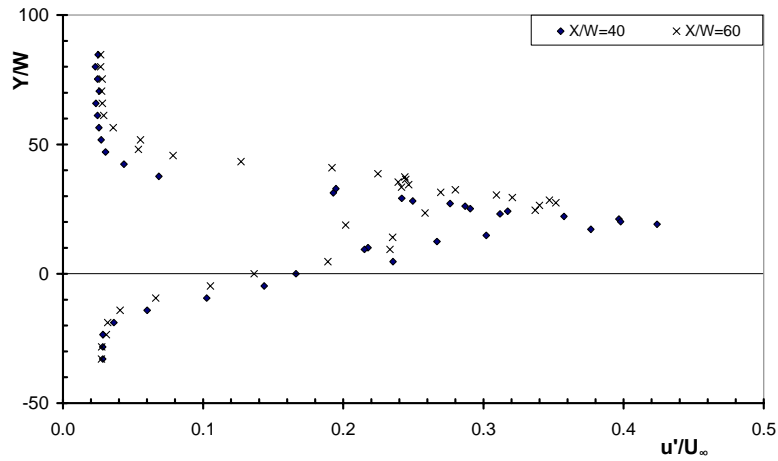


Figure 24 Turbulence streamwise fluctuations downstream the cylinder, $R=8.7$ and $\alpha=60^\circ$. ($X/W=40, 60$)

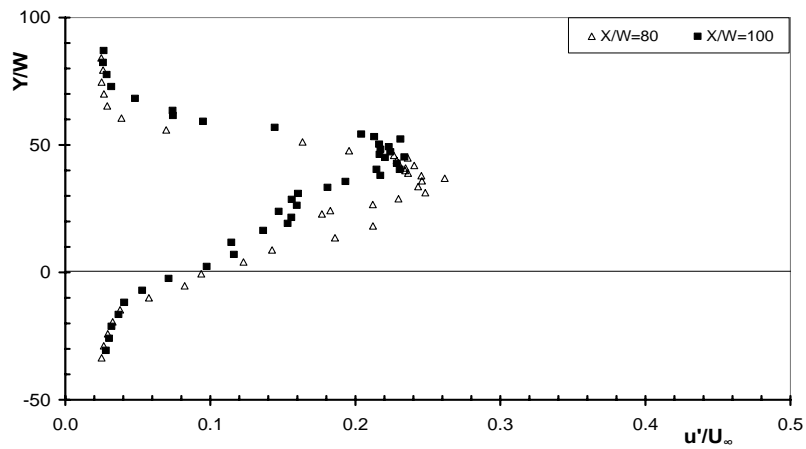


Figure 25 Turbulence streamwise fluctuations downstream the cylinder, $R=8.7$ and $\alpha=60^\circ$. ($X/W=80, 100$)